

Fig. 2 A case of PR after EPI-M-TACE. **a** Computed tomography (CT) revealed a tumor in segment 8. **b** Common hepatic arteriogram revealed a faint tumor stain (*arrow*). Four branches of the anterior superior subsegmental artery of the right hepatic artery (A8) (*arrowheads*) were selectively embolized. **c** CT performed 1 week after TACE revealed dense iodized oil accumulation in the tumor, however, the left-side safety margin was inadequate (*arrow*). **d** CT performed 11 months after TACE revealed PR at the left side where

an adequate safety margin had not been obtained (*arrow*). **e** Follow-up common hepatic arteriogram showed that the embolized branches were severely attenuated and arterioportal shunts had developed. **f** Left hepatic arteriogram revealed that the recurrent tumor was supplied by a branch of the medial subsegmental artery (*arrow*). Arterioportal shunts were also apparent. The *arrowhead* shows the metallic coils placed in A8 to occlude the arterioportal shunts

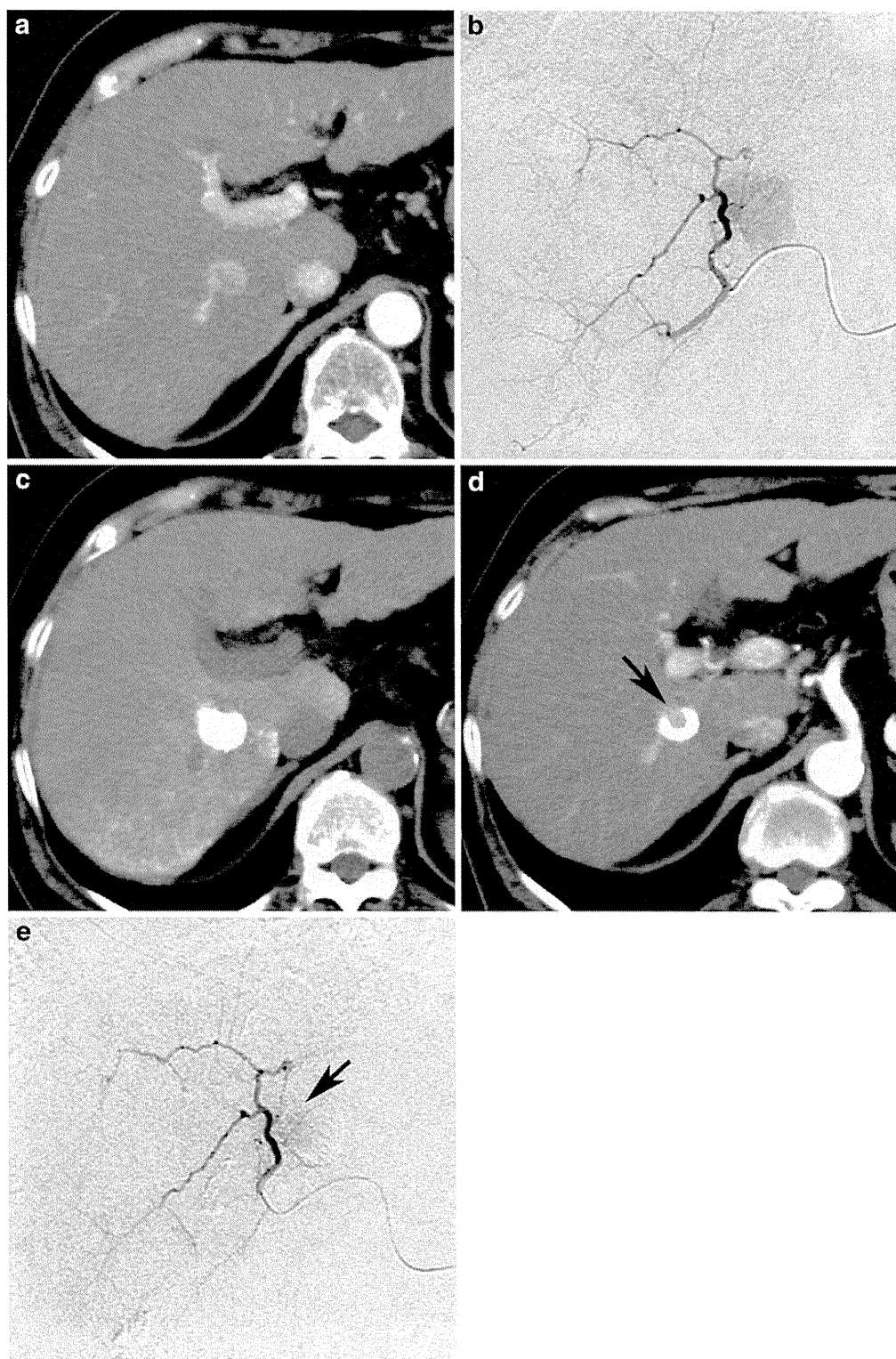


Fig. 3 A case of IR after MPT-I-TACE. **a** CT revealed a small tumor in segment 7. **b** Selective arteriogram of the posterior superior subsegmental artery of the right hepatic artery (A7) revealed a tumor stain. TACE was performed at this point. **c** CT performed 1 week after TACE

showed dense iodized oil accumulation in the tumor. **d** However, CT performed 2 months after TACE revealed IR (*arrow*). **e** Follow-up arteriogram of A7 revealed a tumor stain. In addition, all embolized branches had reopened compared with the initial arteriogram

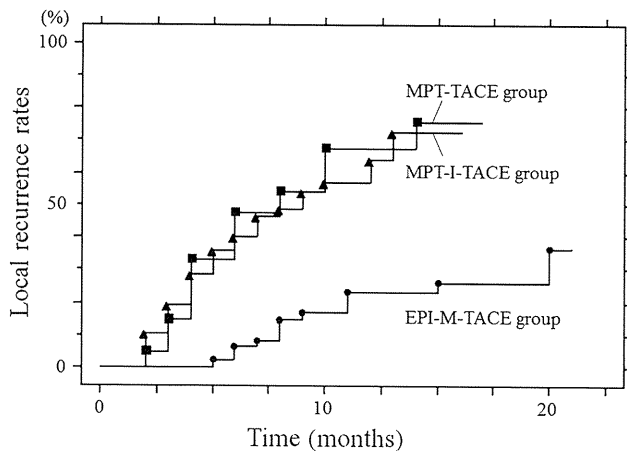


Fig. 4 Plot of cumulative local recurrence in the EPI-M-TACE, MPT-TACE, and MPT-I-TACE groups. Local recurrence in the EPI-M-TACE group was significantly lower than in the MPT-TACE and MPT-I-TACE groups ($P < 0.0001$ and 0.0001 , respectively)

stalled early, because of its high viscosity. In such cases, TACE may have been incomplete because gelatin sponge particles could not be injected adequately. We speculated that the high viscosity of MPT/LPD might be the main cause of IR, and we attempted to reduce the viscosity by mixing contrast material with MPT/LPD to create a water-in-oil (W-O) emulsion, because some authors have reported that hepatic tumor uptake of W-O emulsions was higher than that of pure iodized oil and oil-in-water (O-W) emulsions [16, 17]. However, there were no significant differences in local recurrence between the MPT-I-TACE and MPT-TACE groups and it was still higher than that in the EPI-M-TACE group. Furthermore, the follow-up periods in the MPT-I-TACE group were relatively short, and additional local recurrence, in particular PR, may develop in the future. On the basis of our results, we speculated that the anticancer effect of MPT itself, rather than the type of MPT/LPD, suspension or emulsion, could be the main cause of the very frequent tumor recurrence.

Hamada et al. [6] reported selective distribution and long-term high concentration of platinum in the tumor tissue of the rat liver after injection of MPT/LPD into the hepatic artery. In another experimental study reported by Kishimoto et al. [5], however, only 5.9% of platinum that was initially contained in MPT/LPD was released into saline after 28-days' incubation. This study suggests that the total amount of active platinum released from MPT/LPD is extremely small compared with other hydrophilic anticancer drugs mixed with iodized oil, because these are usually released rapidly from the iodized oil after injection [18, 19].

TACE usually induces arteritis. In addition, development of arterioportal shunts frequently disturbs additional TACE. It is feasible that damage to the hepatic artery by

TACE can be kept to a minimum, to prolong the duration of transcatheter management and avoid reducing the hepatic function reserve [4]. For these reasons, we believe that superselective catheterization is also useful. Follow-up angiograms of the EPI-M-TACE group revealed that all embolized branches were attenuated or occluded. In addition, arterioportal shunts were apparent in 36% of cases. We speculate that superselective EPI-M-TACE severely damages the arteries and this may exaggerate the ischemic effects on tumors. On the other hand, follow-up angiograms after MPT-TACE or MPT-I-TACE showed that almost all embolized branches were reopened and that there were no arterioportal shunts in the embolized areas. This suggests that MPT does not injure the arteries, and that the embolized arteries including the tumor-feeders may recanalize within a few days, owing to absorption of gelatin sponge particles. As a result, the tumor cells that escape exposure to active cytotoxic agents may revive after receiving the restored arterial blood flow. Less damage to the arteries may work as an advantage to preserve hepatic function and to prevent development of extrahepatic collateral pathways to tumors; however, it may also promote tumor recurrence or survival in addition to slow-release of active platinum.

This study has several limitations. First, the study design was not a strict historical control, because between January 2010 and April 2010, both EPI-M-TACE and MPT-TACE were performed and selection of anticancer drugs was not randomized. This could have caused drug selection bias. Second, we know that the objective of TACE is not to achieve local tumor control but to prolong survival. From the results of this study, it could not be determined whether overall survival in the EPI-M-TACE group was superior to that of the MPT-TACE or MPT-I-TACE groups. However, we believe that local control of the tumor may be directly linked to prognosis in patients with inoperable HCC. In addition, it is well known that rapid progression of surviving tumor cells after treatment is rarely observed [20]. Long-term survival of patients in the MPT-TACE or MPT-I-TACE groups is not expected because of very frequent tumor recurrence.

Conclusion

In superselective TACE for HCC, local recurrence in the MPT or MPT-I-TACE groups was significantly higher than in the EPI-M-TACE group. The characteristics of MPT, for example the slow-release of the active platinum compound and less damage to the arteries, may lead to very frequent tumor recurrence, in particular IR, although less arterial damage may work as an advantage to the nontumorous liver.

References

1. Yamada R, Sato M, Kawabata M, Nakatsuka H, Nakamura K, Takashima S. Hepatic artery embolization in 120 patients with unresectable hepatoma. *Radiology*. 1983;148:397–401.
2. Uchida H, Ohishi H, Matsuo N, Nishimine K, Ohue S, Nishimura Y, et al. Transcatheter hepatic segmental arterial embolization using lipiodol mixed with an anticancer drug and Gelfoam particles for hepatocellular carcinoma. *Cardiovasc Intervent Radiol*. 1990;13:140–5.
3. Matsui O, Kadoya M, Yoshikawa J, Gabata T, Arai K, Demachi H, et al. Small hepatocellular carcinoma: treatment with subsegmental transcatheter arterial embolization. *Radiology*. 1993;188:79–83.
4. Miyayama S, Matsui O, Yamashiro M, Ryu Y, Kaito K, Ozaki K, et al. Ultrasensitive transcatheter arterial chemoembolization with a 2-F tip microcatheter for small hepatocellular carcinomas: relationship between local tumor recurrence and visualization of the portal vein with iodized oil. *J Vasc Interv Radiol*. 2007;18:365–76.
5. Kishimoto S, Noguchi T, Yamaoka T, Fukushima S, Takeuchi Y. In vitro release of SM-11355, cis[$((1R, 2R)-1,2\text{-cyclohexanediamine-}N,N')$ bis(myristato)] platinum(II) suspended in lipiodol. *Biol Pharm Bull*. 2000;23:637–40.
6. Hamada M, Baba A, Tsutsumishita Y, Noguchi T, Yamaoka T, Chiba N, et al. Intra-hepatic arterial administration with miriplatin suspended in an oily lymphographic agent inhibits the growth of tumors implanted in rat livers by including platinum-DNA adducts to form and massive apoptosis. *Cancer Chemother Pharmacol*. 2009;64:473–83.
7. Okusaka T, Okada S, Nakanishi T, Fujiyama S, Kubo Y. Phase II trial of intra-arterial chemotherapy using a novel lipophilic platinum derivative (SM-11355) in patients with hepatocellular carcinoma. *Invest New Drugs*. 2004;22:169–76.
8. Ikeda K, Okusaka T, Ikeda M, Morimoto M. Transcatheter arterial chemoembolization with a lipophilic platinum complex SM-11335 (miriplatin hydrate)—safety and efficacy in combination with embolizing agents. *Jpn J Cancer Chemother*. 2010;37:271–5 (in Japanese).
9. Cammà C, Schepis F, Orlando A, Albansese M, Shahied L, Trevisani F, et al. Transarterial chemoembolization for unresectable hepatocellular carcinoma: meta-analysis of randomized controlled trial. *Radiology*. 2002;224:47–54.
10. Kawai S, Okamura J, Ogawa M, Ohashi Y, Tani M, Inoue J, et al. Prospective and randomized clinical trial for the treatment of hepatocellular carcinoma—a comparison of lipiodol-transcatheter arterial embolization with and without adriamycin (first cooperative study). *Cancer Chemother Pharmacol*. 1992;31 Suppl:s1–6.
11. Malagari K, Pomoni M, Kelekis A, Pomoni A, Dourakis S, Spyridopoulos T, et al. Prospective randomized comparison of chemoembolization with doxorubicin-eluting beads and bland embolization with BeadBlock for hepatocellular carcinoma. *Cardiovasc Intervent Radiol*. 2010;33:541–51.
12. Kamada K, Nakanishi T, Kitamoto M, Aikata H, Kawakami Y, Ito K, et al. Long-term prognosis of patients undergoing transcatheter arterial chemoembolization for unresectable hepatocellular carcinoma: comparison of cisplatin lipiodol suspension and doxorubicin hydrochloride emulsion. *J Vasc Interv Radiol*. 2001;12:847–54.
13. Kasai K, Ushio A, Sawara K, Miyamoto Y, Kasai Y, Oikawa K, et al. Transcatheter arterial chemoembolization with a fine-powder formulation of cisplatin for hepatocellular carcinoma. *World J Gastroenterol*. 2010;16:3437–44.
14. Yodono H, Matsuo K, Shinohara A. A retrospective comparative study of epirubicin-lipiodol emulsion and cisplatin-lipiodol suspension for use with transcatheter arterial chemoembolization for treatment of hepatocellular carcinoma. *Anti-Cancer Drugs*. 2011;22:277–82.
15. Kawaoka T, Aikata H, Katamura Y, Takaki S, Waki K, Hiramatsu A, et al. Hypersensitivity reactions to transcatheter chemoembolization with cisplatin and lipiodol suspension for unresectable hepatocellular carcinoma. *J Vasc Interv Radiol*. 2010;21:1219–25.
16. de Baere T, Zhang X, Aubert B, Harry G, Lagrange C, Ropers J, et al. Quantification of tumor uptake of iodized oils and emulsions of iodized oils: experimental study. *Radiology*. 1996;201:731–5.
17. Demachi H, Matsui O, Abo H, Tatsu H. Simulation model based on non-Newtonian mechanics applied to the evaluation of the embolic effect of emulsions of iodized oil and anticancer drug. *Cardiovasc Intervent Radiol*. 2000;23:285–90.
18. Lewis AL, Gonzalez MV, Lloyd AW, Hall B, Tang Y, Willis SL, et al. DC Bead: in vitro characterization of a drug-delivery device for transarterial chemoembolization. *J Vasc Interv Radiol*. 2006;17:335–42.
19. Varela M, Real MI, Burrel M, Forner A, Sala M, Brunet M, et al. Chemoembolization of hepatocellular carcinoma with drug eluting beads: efficacy and doxorubicin pharmacokinetics. *J Hepatol*. 2007;46:474–81.
20. Kojiro M, Sugihara S, Kakizoe S, Nakashima O, Kiyomatsu K. Hepatocellular carcinoma with sarcomatous change: a special reference to the relationship with anticancer therapy. *Cancer Chemother Pharmacol*. 1989;23 Suppl:s4–8.

Main Bile Duct Stricture Occurring After Transcatheter Arterial Chemoembolization for Hepatocellular Carcinoma

Shiro Miyayama · Masashi Yamashiro · Miho Okuda · Yuichi Yoshie ·
Yoshiko Nakashima · Hiroshi Ikeno · Nobuaki Orito · Kazuo Notsumata ·
Hiroyuki Watanabe · Daisy Toyu · Nobuyoshi Tanaka · Osamu Matsui

Received: 7 October 2009 / Accepted: 3 December 2009 / Published online: 8 January 2010
© Springer Science+Business Media, LLC and the Cardiovascular and Interventional Radiological Society of Europe (CIRSE) 2010

Abstract The purpose of this study was to evaluate the clinical course of main bile duct stricture at the hepatic hilum after transcatheter arterial chemoembolization (TACE) for hepatocellular carcinoma (HCC). Among 446 consecutive patients with HCC treated by TACE, main bile duct stricture developed in 18 (4.0%). All imaging and laboratory data, treatment course, and outcomes were retrospectively analyzed. All patients had 1 to 2 tumors measuring 10 to 100 mm in diameter (mean \pm SD 24.5 ± 5.4 mm) near the hepatic hilum fed by the caudate arterial branch (A1) and/or medial segmental artery (A4) of the liver. During the TACE procedure that caused bile duct injury, A1 was embolized in 8, A4 was embolized in 5, and both were embolized in 5 patients. Nine patients (50.0%) had a history of TACE in either A1 or A4. Iodized oil accumulation in the bile duct wall was seen in all patients on computed tomography obtained 1 week later. Bile duct dilatation caused by main bile duct stricture developed in both lobes ($n = 9$), in the right lobe ($n = 3$), in the left lobe ($n = 4$), in segment (S) 2 ($n = 1$), and in S3 ($n = 1$). Serum levels of alkaline phosphatase and γ -glutamyltranspeptidase increased in 13 patients. Biloma requiring drainage developed in 2 patients;

jaundice developed in 4 patients; and metallic stents were placed in 3 patients. Complications after additional TACE sessions, including biloma ($n = 3$) and/or jaundice ($n = 5$), occurred in 7 patients and were treated by additional intervention, including metallic stent placement in 2 patients. After initial TACE of A1 and/or A4, 8 patients (44.4%), including 5 with uncontrollable jaundice or cholangitis, died at 37.9 ± 34.9 months after TACE, and 10 (55.6%) have survived for 38.4 ± 37.9 months. Selective TACE of A1 and/or A4 carries a risk of main bile duct stricture at the hepatic hilum. Biloma and jaundice are serious complications associated with bile duct strictures.

Keywords Hepatocellular carcinoma · Transcatheter arterial chemoembolization · Bile duct stricture · Jaundice · Biloma · Metallic stent placement

Introduction

Transcatheter arterial chemoembolization (TACE) is a widely accepted treatment option for inoperable hepatocellular carcinoma (HCC) [1, 2]. A recent randomized trial showed a distinct survival advantage for TACE compared with the best supportive care [3, 4].

With the advancement of TACE technologies, therapeutic effects have improved, whereas adverse effects have decreased [5–8]. However, TACE may still cause several complications, such as pulmonary oil embolism, abscess formation, tumor lysis syndrome, and intrahepatic bile duct necrosis (biloma), in addition to postembolization syndrome [9–15].

Since the first report by Maciuchi et al. [16], several investigators have reported main bile duct stricture at the

S. Miyayama (✉) · M. Yamashiro · M. Okuda · Y. Yoshie ·
Y. Nakashima · H. Ikeno · N. Orito
Department of Diagnostic Radiology, Fukuiken Saiseikai
Hospital, 7-1, Funabashi, Wadanaka-cho, Fukui 918-8503, Japan
e-mail: s-miyayama@fukui.saiseikai.or.jp

K. Notsumata · H. Watanabe · D. Toyu · N. Tanaka
Department of Internal Medicine, Fukuiken Saiseikai Hospital,
7-1, Funabashi, Wadanaka-cho, Fukui 918-8503, Japan

O. Matsui
Department of Radiology, Kanazawa University Graduate
School of Medical Science, 13-1, Takara-machi,
Kanazawa 920-8641, Japan

hepatic hilum after TACE [17, 18]. However, the causes and clinical futures of bile duct strictures are still not well known. In this report, we describe the clinical course and risk factors for main bile duct stricture at the hepatic hilum after TACE.

Materials and Methods

Patients

Between January 2004 and June 2009, we encountered 18 patients with main bile duct stricture at the hepatic hilum with intrahepatic bile duct dilatation developing after TACE for HCC among 446 consecutive patients treated by TACE. We excluded bile duct invasion of HCC by imaging findings. There were 8 men and 10 women, and the mean patient age was 71.9 ± 6.6 years (range 58 to 83). Patient profiles are listed in Table 1. All patients had liver cirrhosis. This was related to hepatitis C in 13 patients and to hepatitis B in 1 patient. The etiology was unknown in 4 patients. The diagnosis of HCC was established (1) by imaging findings of computed tomography (CT) and/or magnetic resonance imaging (MRI) (i.e., characteristic nodular enhancement on the arterial-phase images and washout on the delayed-phase images) in addition to (2) nodular stain on angiography and/or CT during hepatic arteriography (CTHA) and (3) nodular perfusion defect on CT during arterial portography (CTAP). Since May 2006, CTHA and CTAP images were obtained using a cone-beam CT (CBCT) technique (XperCT; Philips Medical Systems, Best, The Netherlands). The treatment records up to the initial treatment for HCC were retrospectively analyzed. Written informed consent was obtained from each patient before TACE. Institutional Review Board approval for this type of retrospective study is not required at our institution.

TACE Procedure

A 1.8F tip (Carnelian Pixie; Tokai Medical Products, Kasugai, Japan), 2F tip (Progreat α ; Terumo, Tokyo, Japan) or 2.4F tip (Microferret; Cook, Bloomington, IN) microcatheter, passed through a 4F catheter, was used for all TACE procedures. To navigate the microcatheter, a 0.016-inch guidewire (GT-Wire; Terumo) was used. The microcatheter was advanced into the tumor-feeding branch as selectively as possible to minimize the embolized area in each patient.

After the microcatheter was inserted into the target branch, 0.5 mL 2% lidocaine (Xylocaine; Fujisawa, Osaka, Japan) was injected intra-arterially to prevent pain and vasospasm. First, the following was injected a mixture of (1) 2 to 10 mL iodized oil (Lipiodol; Andre Guerbet,

Table 1 Patient profiles

Patient characteristics	
Male	8
Female	10
Mean age (years)	71.9 ± 6.6
Liver cirrhosis (%)	18 (100)
HCV related (%)	13 (72.2)
HB related (%)	1 (5.6)
Etiology unknown (%)	4 (22.2)
Tumor size near the hepatic hilum (mm)	24.5 ± 25.4
Intrahepatic multiplicity (%)	
Single	11 (61.1)
Two	4 (22.2)
Three	1 (5.6)
Four	2 (11.1)

Aulnaysous-Bois, France), (2) contrast material, i.e., 370 mg I/mL iopamidol (Iopamiron 370; Bayer, Osaka, Japan) or 350 mg I/mL iomeprol (Iomeron 350; Ezai, Tokyo, Japan) equal to one third the quantity of iodized oil, (3) anticancer drugs, i.e., 10 to 30 mg epirubicin (Farmorbicin; Kyowa Hakko, Tokyo, Japan), and (4) 2 to 6 mg mitomycin C (Mitomycin; Kyowa Hakko)—followed by injection of gelatin sponge particles. The total amount of iodized oil in a single procedure was determined based on tumor size (almost equal to the diameter of the tumor, e.g., a 3-cm tumor received 3 mL iodized oil) but did not exceed 10 mL in a single TACE session. Up until December 2006, we had used gelatin sponge (Gelfoam; Upjohn, Kalamazoo, MI) particles cut into approximately 1-mm cubes. Since January 2007, we have used commercially available 1 mm-diameter gelatin sponge particles (Gelpart; Nippon Kayaku, Tokyo, Japan). For all patients but 2, the particles were crushed into approximately 0.5-mm particles by pumping 20 times using a 3-way stopcock and 2 2.5-mL syringes, and then the gelatin sponge slurry was injected to obstruct the tumor-feeding branch. In the remaining 2 patients, who had tumors measuring 9.3 and 10 cm in diameter, respectively, 1-mm diameter gelatin sponge particles were used. Gelatin sponge particles were injected until the tumor-feeding branch was blocked and the targeted tumor stain disappeared on angiography. In addition, stepwise TACE sessions were performed at 3-to 10-week intervals to avoid severe complications, such as abscess formation or tumor lysis syndrome.

CBCT was performed in 7 patients during the TACE procedure. In 3 patients, CBCT images were obtained by injection of contrast material through A1 ($n = 2$) or immediately after TACE of both A1 and the medial segmental artery (A4) ($n = 1$) to confirm the embolized area.

Follow-Up

Unenhanced CT was obtained at 1 week after TACE in all patients to check for iodized oil distribution. All patients were followed-up, and dynamic CT was performed every 2 to 3 months after TACE to investigate any tumor recurrence. If possible, an additional TACE session was performed when local recurrence or newly developed lesions were demonstrated at other sites. MRI ($n = 11$), endoscopic retrograde cholangiopancreatography (ERCP) ($n = 8$), or percutaneous transhepatic biliary drainage (PTBD) ($n = 6$) was performed when main bile duct stricture with bile duct dilatation was demonstrated on follow-up CT. Laboratory data—including serum bilirubin (normal range 0.2 to 1.0 mg/dL), alkaline phosphatase (ALP; normal range 104 to 338 U/L), and γ -glutamyl-transpeptidase (γ -GTP; normal range 16 to 73 U/L)—were examined in all patients 1 day before TACE, 1 week after TACE, and every 1 to 3 months after TACE. Degrees of increased ALP level were divided into 3 grades: slight (<150 U/L), moderate (151 to 300 U/L), and marked (>301 U/L). Degrees of increased γ -GTP level were also divided into 3 grades: slight (<100 U/L), moderate (101 to 200 U/L), and marked (>201 U/L).

Data Analysis

All imaging results (arteriograms, CBCT, CT, MRI, cholangiograms), laboratory data, treatment courses, and outcomes were retrospectively evaluated in each patient.

Results

The results are summarized in Table 2. All patients were followed-up until death or to date.

Tumors

Eleven patients had a single tumor, and 7 patients had 1 to 3 tumors. All patients but 1 had a tumors in S1 and/or S4. The remaining patient had a tumor protruding from S2, which was partially supplied by A1. Five patients had a tumor located in S1, including 1 patient with 2 tumors in S1. Five patients had a tumor located in S4. Four patients each had a tumor located in the boundary between S4 and S5, between S1 and S4, between S1 and S8, and between S1 and S5. Two patients had a large tumor located in the right lobe extending to S1 and S4. One patient had 2 tumors located in both S1 and S4. In total, 20 tumors were located near the hepatic hilum. All were initially detected HCCs without any previous treatment ($n = 9$) or new HCCs in patients who had a history of previous treatment for HCC ($n = 11$). Mean

tumor diameter was 24.5 ± 25.4 mm (range 10 to 100). Six patients had 1 to 3 other small viable tumors with a mean diameter of 1.7 ± 1.0 mm at the periphery of the liver.

Embolized Branches

All patients underwent TACE of A1 and/or A4 during the TACE procedure just before development of bile duct stricture. Three patients underwent TACE of A1 alone, and 5 patients underwent TACE of A1 and other hepatic branches except A4 (Figs. 1, 2), including 2 patients who underwent embolization of 2 A1 branches. Five patients underwent TACE of A4 and other hepatic branches except A1, including 1 patient who underwent embolization of 2 A4 branches (Fig. 3). Three patients underwent TACE of both A1 and A4. The remaining 2 patients underwent TACE of both A1 and A4, in addition to another hepatic arterial branch or extrahepatic collaterals. In total, A1 was embolized in 8 patients; A4 was embolized in 5 patients; and both A1 and A4 were embolized in 5 patients. During the TACE procedure, communications between the following were demonstrated: the right A1 and the left A1 ($n = 3$), the A1 and the A4 ($n = 2$), 2 A4 branches ($n = 2$), and the A1 and the 3 o'clock and 9 o'clock arteries ($n = 2$) (Figs. 1, 4). In 9 patients (50.0%), TACE of A1 and/or A4 had previously been performed. TACE of A1 had been performed once in 2 patients. TACE of A4 had been performed once in 2 patients and twice in 1 patient. TACE of both A1 and A4 had been performed in 4 patients, including 3 patients who had undergone TACE of 2 A1 branches and 2 A4 branches once to 3 times.

Among 446 consecutive patients treated by TACE during the same period, A1 was embolized in 54 patients; A4 was embolized in 152 patients; and both A1 and A4 were embolized in 86 patients. Thus, the incidence of bile duct stricture after TACE was 4.0% and that after TACE of A1 and/or A4 was 6.2%.

CBCT Findings Obtained During the Procedure

CBCT during arteriography of A1 showed wall enhancement of the common hepatic duct (CHD) in 1 patient (Fig. 1) and wall enhancement of the CHD and right hepatic duct (RHD) in another patient (Fig. 2). CBCT obtained immediately after TACE of both A1 and A4 showed iodized oil accumulation in the wall of the left hepatic duct (LHD).

CT Findings Obtained 1 Week After TACE

Iodized oil accumulation in the CHD wall was seen in 9 patients (50%), 4 with TACE of both A1 and A4, 4 with TACE of A1, and 1 with TACE of A4 (Figs. 1, 2). It

Table 2 Summary of 18 patients with main bile duct stricture occurring after TACE

Case no./age (years)/sex	Tumor diameter (mm)	Segment	Embolized branches	Anastomosed branches	Previous embolized branches (no. of times)	Iodized oil-accumulated portion	Site of bile duct dilatation	Shrinkage of gallbladder	Changes in bile duct dilatation	Complications	No. of additional TACE	Complications after additional TACE
1/80/F	19	S4	A4, etc.		A4 (1)	LHD	Both	+	Progressed	Biloma	1	Jaundice
2/76/F	16	S1	A1			CHD	Both	+	Progressed		1	
3/72/M	20	S2, etc.	A1 × 2, etc.	A1–A1		LHD	Left	+	Progressed		4 ^c	
4/81/F	10	S1	A1			CHD	Right		Improved	Cholangitis	1	Biloma
5/61/F	10	S1	A1	A1–A4	A1 (1)	RHD	Right		Progressed			
6/74/M	20	S1/4, etc.	A1, A4	A4–A4		CHD	Both		Improved	Cholangitis, biloma,		
7/64/M	17	S1	A1, etc.		A1 (3), A4 (2)	CHD	Both		Progressed	Jaundice ^a	4	Biloma, jaundice ^d
8/58/M	100	S8-1-4	A4, etc.	A1–A1	A1 (2), A4 (1)	CHD	Both		Progressed	Biloma ^b , jaundice ^a ,	2	Biloma ^b
9/83/F	93	S8-1-4	A1, A4, etc.	A1–3 and 9 o'clock As	A1 (3), A4 (1)	CHD	Both		Improved	Biloma	4	
10/73/F	16	S4	A1, A4, etc.	A1–A1	A4 (1)	CHD	Left		Progressed		3	Jaundice ^a
11/70/M	24, 12	S1, etc.	A1 × 2, etc.			CHD	Both			Jaundice		
12/71/F	12	S1/8, etc.	A1, etc.			LHD	S2		Progressed		1	
13/68/F	17	S4, etc.	A4 × 2, etc.			LHD	S3		Progressed		5	
14/70/M	36	S4/5	A4, etc.		A1 (1), A4 (2)	CHD, RHD, LHD	Both		Progressed	Biloma ^b , jaundice ^a	1	Jaundice ^d
15/76/M	11	S4 × 2, etc.	A4, etc.	A4–A4		CHD, LHD	Left		Progressed		3	
16/77/F	17	S5/1	A1, etc.	A1–3 and 9 o'clock As	A1 (1)	RHD, CHD, CBD	Right	+	Progressed			
17/68/M	15	S4	A1, A4	A1–A4	A4 (2)	CHD	Both		Progressed		4	Jaundice ^a
18/72/F	10, 15	S1, S4	A1, A4			LHD	Left					

^a Percutaneous transhepatic biliary drainage and stent placement was performed

^b Percutaneous drainage was performed

^c Metallic stent was placed to relief bile duct stricture before additional TACE

^d Percutaneous transhepatic biliary drainage was continued until patients' death



Fig. 1 A 74-year-old man with HCC in S1/4 (patient no. 6). **A** Right hepatic arteriogram shows A1 arising from the proximate portion of the anterior branch of the right hepatic artery (*arrow*). **B** CBCT during arteriography of A1 shows wall enhancement of the CHD (*arrow*). This vessel was embolized. **C** Spot radiograph obtained during TACE of A1. **D** Left hepatic arteriogram shows 2 A4 branches (*arrows*). **E** One A4 branch was selected and embolized. During the TACE procedure, another A4 branch is demonstrated through anastomosis (*arrow*). The *arrowhead* indicates a tumor. **F** CT obtained at 1 week

after TACE shows iodized oil accumulation and wall thickening of the CHD (*arrow*). **G** CT obtained 1 month after TACE shows wall thickening of the CHD and intrahepatic bile duct dilatation. **H** ERCP shows the stricture at the CHD (*arrow*) and occlusion of the LHD. Intraluminal defect suggesting coagula in the CHD is also seen (*arrowhead*). **I** CT obtained at 3 months after TACE shows improvement of bile duct wall thickening and intrahepatic bile duct dilatation

was seen in the LHD wall in 5 patients (27.8%), in 1 patient with TACE of both A1 and A4, in 2 patients with TACE of A1, and in 2 patients with TACE of A4 (Fig. 3). It was seen in the RHD wall in 1 patient (5.6%) with TACE of A1. It was seen in the LHD wall and CHD wall in 1 patient (5.6%) with TACE of A4 and in the bilateral hepatic ducts wall and CHD wall in 1 patient (5.6%) with TACE of A4. In 1 patient (5.6%) with demonstration of the 3 o'clock and 9 o'clock

arteries during TACE of A1, iodized oil was accumulated in the RHD, the CHD, and the CBD (Fig. 4). Bile duct wall thickening at the site of iodized oil accumulation was also demonstrated in all patients (Figs. 2, 3, 4, 5). In all 3 patients who underwent selective CBCT, CT obtained 1 week after TACE showed iodized oil accumulation in the same portion of the bile duct where wall enhancement or iodized oil accumulation was observed on CBCT (Fig. 1).

Fig. 2 An 81-year-old woman with HCC in S1 (patient no. 4). **A** Arteriogram of A1 shows a faint tumor stain (*arrow*). **B** CBCT during arteriography of A1 shows a tumor stain (*arrow*). Wall enhancement of the CHD and RHD is also seen (*arrowheads*). **C** CT obtained at 2 months after TACE of A1 shows wall thickening of the CHD (*arrow*) and intrahepatic bile duct dilatation (not shown). **D** MR cholangiopancreatography shows short and smooth strictures at the CHD and RHD (*arrows*). Intraluminal defect suggesting coagula is also seen (*arrowhead*)



In patients who underwent repeated TACE sessions of A1 and/or A4, iodized oil accumulation was observed at the same portion of the bile duct on each CT obtained 1 week after the respective TACE procedures.

Serial CT Findings

Main bile duct stricture at the hepatic hilum and intrahepatic bile duct dilatation developed in all patients. Except for 1 patient, the site of bile duct stricture corresponded with the portion showing iodized oil accumulation on CT obtained at 1 week after TACE. In this 1 patient, CT obtained at 1 week after TACE showed iodized oil accumulation in the RHD, the CHD, and the CBD wall, but the stricture developed only at the RHD. Bile duct dilatation was seen in both lobes ($n = 9$ [50.0%]) (Fig. 1), in the right lobe ($n = 3$ [16.7%]) (Fig. 4), in the left lobe ($n = 4$ [22.2%]), in S2 ($n = 1$ [5.6%]), and in S3 ($n = 1$ [5.6%]) (Fig. 3). These findings were demonstrated after initial TACE of A1 and/or A4 in 9 patients (50.0%) and after 2 to 4 TACE sessions of A1 and/or A4 in 9 patients (50.0%). The findings were demonstrated 4 to 92 months (mean

32.6 ± 29.7) after the initial TACE of A1 and/or A4 and 2 to 4 months (mean 2.8 ± 0.8) after the last TACE of A1 and/or A4 before bile duct injury. In 5 patients (27.8%), hyperattenuating material suggesting coagula was seen in the CBD. Intrahepatic biloma developed simultaneously in 5 patients (27.8%).

During follow-up, bile duct dilatation improved in 3 patients (16.7%) (Fig. 1), whereas it gradually progressed in 13 patients (72.2%) (Fig. 4). In the remaining 2 patients (11.1%), follow-up CT was not obtained except for the CT that initially demonstrated the bile duct dilatation. In addition, shrinkage of the gallbladder and retention of concentrated bile developed in 4 patients (22.2%) (Fig. 4).

MRI Findings

MRI was obtained in 11 patients. Strictures of the CHD and bilateral hepatic ducts were seen in 7 patients (63.6%); strictures of the CHD and RHD were seen in 2 patients (18.2%) (Fig. 2); and stricture of the LHD was seen in 2 patients (18.2%). Intraluminal coagula was seen in 8 patients (72.7%) (Fig. 2).

Fig. 3 A 68-year-old woman with HCC in S4 (patient no. 13). **A** Proper hepatic arteriogram shows a tumor supplied by 2 A4 branches (*arrows*). **B** One A4 branch was selected and embolized. **C** Another A4 branch was subsequently selected and embolized. **D** CT obtained at 1 week after TACE shows iodized oil accumulation in the tumor and LHD (*arrow*). **E** CT obtained at 72 months after TACE shows marked bile duct dilatation in S3 without any clinical symptoms. Iodized oil is also densely retained in the tumor (*arrow*)

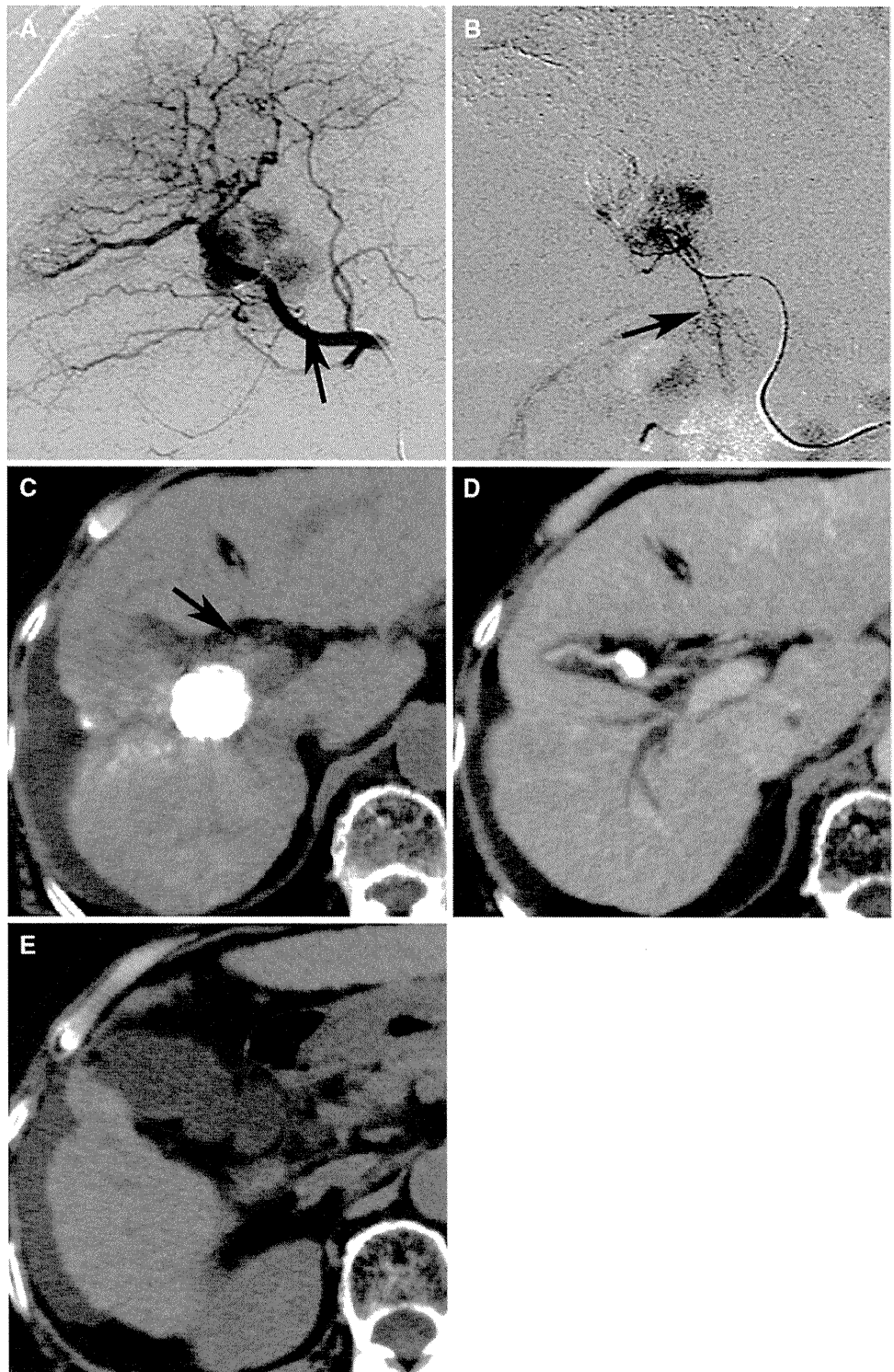


ERCP and PTBD Findings

ERCP was performed in 8 patients, and PTBD was performed in 6 patients. Two patients underwent both examinations. ERCP showed occlusion of the CHD in 2 patients (25.0%): occlusion of the RHD in 1 patient (12.5%) and

occlusion of the LHD in 1 patient (12.5%). In 3 patients (37.5%), strictures of the CHD and bilateral hepatic ducts were seen. In the remaining patient (12.5%), strictures of the CHD and RHD and occlusion of the LHD were seen (Fig 2). Intraluminal defects suggesting coagula were seen in 6 patients (75.0%) (Fig. 1).

Fig. 4 A 77-year-old woman with HCC in S1/S5 (patient no. 16). **A** Right hepatic arteriogram shows a tumor stain supplied by the anterior branch of the right hepatic artery and A1 (*arrow*). Another A1 arising from the right hepatic artery was previously embolized (not shown). **B** Arteriogram of A1 shows a tumor stain. The 3 o'clock and 9 o'clock arteries that are not seen on (A) are also demonstrated (*arrow*). **C** CT obtained at 1 week after TACE shows iodized oil accumulation in the tumor and RHD (*arrow*). Iodized oil is also accumulated in the CHD and CBD (not shown). **D** CT obtained at 6 months after TACE shows intrahepatic bile duct dilatation in the right lobe of the liver. The gallbladder markedly shrinks and concentrated bile is retained. Gallstone is also seen. **E** CT obtained before TACE shows a normal appearance of the gallbladder without gallstone



PTBD was performed under sonographic guidance. The transhepatic approach was performed from the left in 4 patients and bilaterally in 2 patients. Four patients (66.7%) showed strictures of the bilateral hepatic ducts (Fig. 5); 1 patient (16.7%) showed stricture of the CHD; and 1 patient

(16.7%) showed stricture of the LHD. Intraluminal defects suggesting coagula were seen in 4 patients (66.7%). In all patients, the occluded or stenotic segment was relatively short and smooth on cholangiography obtained by MRI, ERCP, and/or PTBD (Figs. 2, 5).

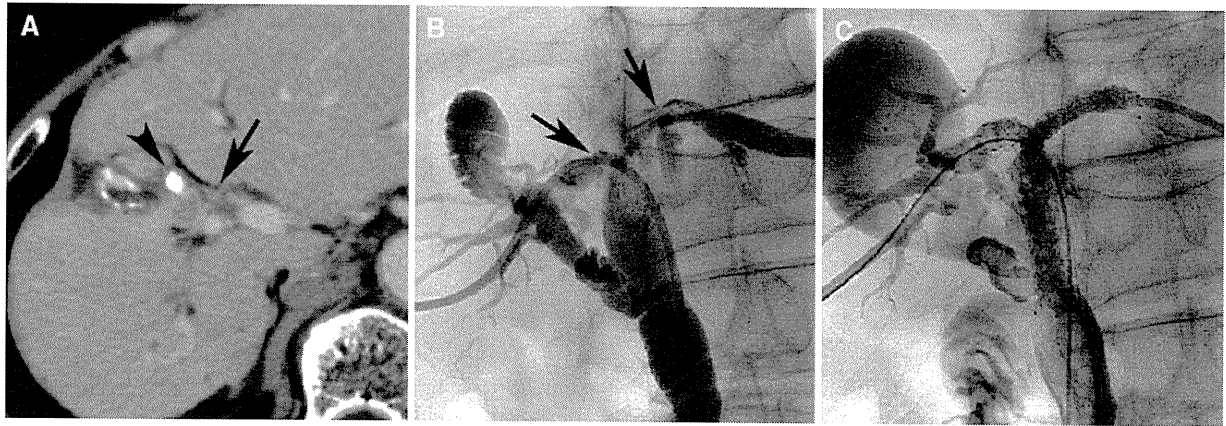


Fig. 5 A 68-year-old man with bile duct strictures at the hepatic hilum (patient no. 17). **A** CT obtained before the additional fourth TACE session (at 22 months after demonstration of bile duct dilatation) shows the stricture and wall thickening of the CHD (*arrow*) in addition to intrahepatic bile duct dilatation. The *arrowhead*

indicates an iodized oil accumulated tumor. **B** This patient presented with jaundice 2 weeks after the additional fourth TACE and PTBD was performed. Cholangiogram obtained through the PTBD catheter shows strictures at the bilateral hepatic ducts and CHD (*arrows*). **C** Two metallic stents were placed by way of a bilateral approach

Changes in Laboratory Data After TACE

Before TACE, serum ALP level was high in 6 patients, and γ -GTP level was high in 5 patients. Serum ALP levels increased in 13 patients (72.2%) from 345.1 ± 89.6 U/L (range 244 to 591) to 582.1 ± 198.7 U/L (range 378 to 1083) at 1 week to 14 months (mean 3.7 ± 4.1) after the last TACE session before bile duct dilatation. Five patients were classed as showing a slight increase, 3 as having a moderate increase, and 5 as having a marked increase. In 1 patient with a slight increase and in all 5 patients with a marked increase, jaundice developed during the follow-up period. Cholangitis developed in 1 patient showing a moderate increase. In the same patients, serum γ -GTP levels increased from 71.8 ± 57.8 U/L (range 29 to 233) to 245.2 ± 169.3 U/L (range 107 to 604) at 1 week to 14 months (mean 4.2 ± 3.9) after the last TACE before bile duct dilatation. Five patients were classed as showing a slight increase, 4 as having a moderate increase, and 4 as having a marked increase. The grades of increase in ALP and γ -GTP were well correlated. Jaundice developed in 1 patient with a slight increase, in 2 patients with a moderate increase, and in 3 patients with a marked increase. Cholangitis developed in 1 patient showing a marked increase. In 9 of 13 patients, serum levels of these enzymes gradually increased. In 5 patients (27.8%), there were no remarkable changes despite bile duct dilatation in the right lobe ($n = 3$), in S2 ($n = 1$), and in S3 ($n = 1$).

Clinical Courses and Outcomes

All patients were followed-up for 3 to 129 months (mean 38.2 ± 35.4) after the initial TACE of A1 and/or A4 and

for 3 to 72 months (mean 25.2 ± 17.6) after the last TACE before bile duct dilatation. Eleven patients (61.1%) presented with bile duct complications associated with main bile duct stricture. Cholangitis developed in 2 patients (11.1%) at 2 months after TACE and resolved after administration of antibiotics (Sulperazon; Pfizer, Tokyo, Japan). Bile duct dilatation was improved during follow-up in these patients (Fig. 1). Biloma developed in 4 patients (22.2%), and percutaneous drainage was performed in 2 of 4 patients at 2 and 4 months, respectively, after the last TACE before bile duct dilatation.

Jaundice (serum bilirubin level 9.3 to 14.0 mg/dL [mean 11.7 ± 2.3]) developed in 4 patients (22.2%), including 2 with a history of biloma drainage, at 5 to 11 months (mean 7.3 ± 2.9) after the last TACE before bile duct dilatation. Three patients underwent PTBD. In the remaining patient, bile duct drainage was not performed because of the patient's poor general condition. In another patient without jaundice, PTBD was performed to relieve bile duct dilatation before additional TACE with bile duct dilatation for HCC in the left lobe of the liver. Metallic stent placement (Zilver 635; Cook) was subsequently performed in 4 patients. In 2 patients, 2 metallic stents were placed from the bilateral hepatic ducts to the CBD using either a bilateral or left approach. In 2 patients, 1 metallic stent was placed from the LHD to CHD by way of a left approach. The PTBD catheter was removed after stent placement.

In 13 patients (72.2%), including 4 who underwent stent placement, 1 to 5 additional TACE sessions (mean 2.6 ± 1.5) were performed because of local recurrence and/or new lesions at other sites. In total, 24 TACE sessions to the area with bile duct dilatation or stented lobe were performed in 12 patients, and 10 TACE sessions to

the area without bile duct dilatation were performed in 5 patients.

Complications associated with additional TACE sessions occurred in 7 of 13 patients (53.8%). Biloma developed in 3 patients. It developed in 2 patients at 2 months after the additional first TACE session to the area with bile duct dilatation or stented lobe and in 1 patient at 1 month after 4 additional TACE sessions to the stented lobe. Percutaneous drainage was required in 1 patient with previous stent placement. Jaundice (6.5 to 22.6 mg/dL [mean 12.6 ± 6.7]) developed in 5 patients at 3 to 26 months (mean 15.4 ± 19.7) after the first additional TACE session and at 2 weeks to 5 months (mean 2.8 ± 1.8) after the last additional TACE session, including 2 patients who had undergone stent placement. It developed after 1 ($n = 2$), 3 ($n = 1$), and 4 ($n = 2$) additional TACE sessions to the area with bile duct dilatation ($n = 3$) or to the stented lobe ($n = 2$). One of these patients also had a small biloma. All patients but 1 underwent PTBD. In 1 patient, 1 metallic stent was placed from the LHD to CBD using a left approach. In another patient, 2 metallic stents were placed from the bilateral hepatic ducts to CBD using a bilateral approach (Fig. 5). The bile duct was occluded in the stented segment in 2 patients who had previously undergone stent placement. Jaundice did not improve because of hepatic failure, and external drainage was continued until the patients' death. In the remaining patient, PTBD was not performed because of the patient's poor general condition. Cholangitis recurred in 1 patient at 1 month after stent placement without an additional TACE session, and it did not improve despite administration of antibiotics. One patient who had undergone stent placement to relieve bile duct stricture before additional TACE sessions did not develop any complications despite 4 additional TACE sessions, including 2 to the stented lobe.

Seven patients (38.9%) have not presented any symptoms for 3 to 68 months (mean 28.6 ± 24.3) since the development of bile duct stricture, and 3 patients (16.7%) including 2 who underwent metallic stent placement have not shown any symptoms associated with bile duct stricture for 3 to 17 months (mean 9.0 ± 7.2) since the additional intervention.

Eight patients (44.4%), including 3 who underwent stent placement ($n = 5$), died of hepatic failure ($n = 2$), uncontrollable jaundice, cholangitis, and/or tumor progression ($n = 1$) at 11 to 119 months (mean 37.9 ± 34.9) after the initial TACE of A1 and/or A4 and at 11 to 41 months (mean 21.3 ± 10.4) after the last TACE session before bile duct dilatation. Ten patients (55.6%) have survived 3 to 129 months (mean 38.4 ± 37.9) after the initial TACE of A1 and/or A4 and 3 to 72 months (mean 28.4 ± 21.9) after the last TACE session before bile duct dilatation. Four patients have not shown any viable HCCs,

but 6 patients have viable HCCs despite repeated TACE sessions.

Discussion

TACE plays an important role in the treatment of unresectable HCC [1–8]. However, several complications associated with TACE have been reported [9–18]. Main bile duct necrosis, followed by stricture, is one of the severe complications of TACE [16–18]. The liver is dually supplied by hepatic arterial and portal venous blood, whereas HCC is mainly supplied by arterial blood. When the tumor-feeding hepatic arterial branch is blocked, the tumor may develop ischemic necrosis, whereas the normal liver may only be slightly affected [1]. However, the biliary tree is supplied primarily by arterial blood alone [19]; therefore, it may be damaged by TACE. Chronic inflammation eventually leads to extensive focal fibrosis of large bile ducts [17].

The extrahepatic and intrahepatic bile ducts are surrounded by a vascular plexus, which is composed of branches arising directly from the right and left hepatic arteries and their segmental branches and indirectly from the gastroduodenal artery by way of the arteries supplying the CBD [20, 21]. The plexus around the RHD and LHD is continuous, with a similar plexus surrounding the CBD and CHD. This intrahepatic plexus is always closely associated with the arterial supply of S1, and A1 gives several branches to the hepatic duct plexus [20].

There is a communicating arcade between the right and left hepatic arteries. This arcade originates mainly from A4 on the left side and from the anterior branch of the right hepatic artery or the right hepatic artery on the right side and supplies S1 and the hilar bile duct [22]. Vellar [23] also reported that A4 is the most important blood supply to the LHD. We speculate that the right branch of the communicating artery, which was described in a report by Tohma et al. [22], might have been A1 in our previous report [24]. When embolic materials are injected into 1 of these vessels, they may flow into another vessel through this communication. In the present study, communications between A1 and A4, between A1 and the 3 o'clock and 9 o'clock arteries, and between two separate branches of A1 or A4 were also demonstrated during the TACE procedure. These communications may explain frequent iodized oil inflow in the posterior aspect of S4 seen on CT obtained after TACE of A1 [24].

Kim et al. [17] reported that focal strictures at the CHD level, or in hepatic ducts adjacent to the CHD level, were seen in their series of bile duct injury by TACE. In the present study, all strictures were also located at the CHD and/or the RHD or the LHD. This may reflect the vascular

supply of the CHD and bilateral hepatic ducts from the hepatic arterial branches, including A1 and A4, whereas the CBD is mainly supplied by the branches of the gastroduodenal artery [20, 21]. The poor collateral supply to the CHD, compared with a denser arterial network and a relatively high proportion of supply to the lower CBD, could explain the vulnerability of the CHD to ischemic injury [21]. All strictures were focal and smooth, and intraluminal coagula was frequently detected on CT, MRI, and cholangiogram. We consider that these findings may be typical image findings of bile duct injury by TACE. Radiologists should not misdiagnose this condition as bile duct invasion by the tumor.

Kobayashi et al. [19] reported that TACE or hepatic arterial infusion chemotherapy might cause reduction of the inner layer vessels of the peribiliary capillary plexus. Kim et al. [17] and Bang et al. [18] also reported that repeated TACE sessions were a risk factor for ischemic bile duct injury. In the present study, all main bile duct strictures developed after TACE of A1 and/or A4. In addition, 50% of bile duct strictures developed even after a single TACE session of A1 and/or A4, suggesting that selective TACE of A1 and/or A4 is a main cause of bile duct necrosis. However, nonselective TACE of the right hepatic artery or left hepatic artery level may mainly damage “the peripheral branches,” whereas “the central branches,” such as A1 and A4, may be slightly damaged or occasionally preserved. Repeat TACE sessions may finally damage these central branches because the peripheral branches are severely attenuated by previous TACE procedures, and embolic materials flows mainly into these central branches.

Makuuchi et al. [16] reported that the intrahepatic and extrahepatic bile ducts would become necrotic if small particles $<250\ \mu\text{m}$ were used. In a report by Chen et al. [21], the artery that supplies the RHD and the LHD has an average diameter of $0.33 \pm 0.15\ \text{mm}$. In the present study, gelatin sponge particles approximately 0.5 to 1 mm in diameter caused bile duct injury, although there was a possibility of contamination by small fragments $<250\ \mu\text{m}$. We speculate that selective TACE of A1 and/or A4 presents a risk of developing bile duct stricture regardless of the size of gelatin sponge particles. The incidence of main bile duct necrosis by selective TACE of A1 and/or A4 was approximately 6% in the present study. This incidence may have been influenced by the magnitude of TACE, the position of the catheter tip, the patterns of arterial supply of the main bile duct, and the damage to the peribiliary plexus and collaterals by previous TACE sessions. In addition, the presence of multiple branches of A1 and A4 may salvage bile duct ischemia by acting as collateral circulation [25]. We speculate that the use of smaller particles may not significantly increase the incidence of main bile duct

stricture, except when these are selectively injected into A1 and/or A4.

With advancements in catheter and guidewire technology, it has become possible to introduce a microcatheter into small branches of the hepatic artery [5–8]. Iodized oil and gelatin sponge particles injected with slight force through the microcatheter may distribute more distally rather than corresponding with natural arterial blood flow [8]. We reported that ultraselective TACE has strong therapeutic effects to achieve not only complete tumor necrosis but also massive peritumoral necrosis by blockage of both the hepatic arterial and portal blood flow [26]. During selective TACE of A1 and/or A4, injection of embolic materials with slight force may increase the risk of bile duct necrosis because embolic materials may flow into the vascular plexus around the main bile ducts directly or indirectly through anastomosis. Chen et al. [21] reported that the marginal artery of the CHD connects with the cystic artery. We speculate that embolic materials injected from A1 or A4 may also flow into the cystic artery through the anastomosis, and thus shrinkage of the gallbladder may occur; this was observed in 22% of patients in the present study.

It may be difficult to predict main bile duct injury by TACE. In 3 patients undergoing selective CBCT during the TACE procedure of A1 and/or A4, bile duct wall enhancement was clearly demonstrated. CBCT might be useful for predicting bile duct injury caused by TACE. We should always bear in mind that selective TACE of A1 and/or A4 carries the risk of causing bile duct necrosis. Therefore, complete blockage of these vessels should be avoided, especially when bile duct enhancement is seen on CT or CBCT during arteriography through A1 or A4. In addition, distal advancement of a thinner microcatheter with a tip $<2\text{F}$ into A1 or A4 may be useful to avoid embolization of small vessels supplying the main bile ducts because these vessels may be estimated to arise from the proximate portion of A1 and A4. CT obtained at 1 week after TACE may also be useful to suggest main bile duct damage. Changes in laboratory data are not sufficiently sensitive, and abnormalities may become apparent long after demonstration of bile duct dilatation on CT in most patients, although marked changes suggest severe damage to the main bile ducts.

Optimal management of main bile duct stricture occurring after TACE has not yet been established. In previous reports, surgical resection was performed when jaundice developed [16–18]. In the present study, we treated 6 patients using metallic stents. Cholangitis and jaundice recurred in 3 patients after stent placement, including 2 who underwent repeated TACE sessions to the stented segment. In addition, a large biloma developed in 1 patient after an additional TACE session performed after stent

placement. Metallic stent placement may be useful to manage main bile duct stricture caused by TACE because patients with inoperable HCC are not good candidates for surgical bile duct repair. However, bile duct complications may occur at high rates after additional TACE sessions. In addition, we should be well aware that intrahepatic bile duct dilatation is a significant risk factor in developing biloma after TACE [15].

In conclusion, selective TACE of A1 and/or A4 presents a risk of causing main bile duct stricture at the hepatic hilum regardless of the number of TACE sessions and the particle size of the embolic material. Focal and smooth bile duct strictures mainly at the CHD are characteristic findings, and intraluminal coagula are frequently detected on CT, MRI, and cholangiography. Radiologists should well aware this uncommon but severe complication of TACE.

References

1. Yamada R, Sato M, Kawabata M et al (1983) Hepatic artery embolization in 120 patients with unresectable hepatoma. *Radiology* 148:397–401
2. Takayasu K, Arri S, Ikai I et al (2006) Prospective cohort study of transarterial chemoembolization for unresectable hepatocellular carcinoma. *Gastroenterology* 131:461–469
3. Llovet JM, Real MI, Montana X et al (2002) Arterial embolisation or chemoembolisation versus symptomatic treatment in patients with unresectable hepatocellular carcinoma: a randomized controlled trial. *Lancet* 359:1734–1739
4. Lo CM, Ngan H, Tso WK et al (2002) Randomized controlled trial of transarterial lipiodol chemoembolization for unresectable hepatocellular carcinoma. *Hepatology* 35:1164–1171
5. Uchida H, Ohishi H, Matsuo N et al (1990) Transcatheter hepatic segmental arterial embolization using Lipiodol mixed with an anticancer drug and Gelfoam particles for hepatocellular carcinoma. *Cardiovasc Intervent Radiol* 13:140–145
6. Matsui O, Kadoya M, Yoshikawa J et al (1993) Small hepatocellular carcinoma: treatment with subsegmental transcatheter arterial embolization. *Radiology* 188:79–83
7. Takayasu K, Muramatsu Y, Maeda T et al (2001) Targeted transarterial oily chemoembolization for small foci of hepatocellular carcinoma using a unified helical CT and angiography system: analysis of factors affecting local recurrence and survival rates. *AJR Am J Roentgenol* 176:681–688
8. Miyayama S, Matsui O, Yamashiro M et al (2007) Ultrasensitive transcatheter arterial chemoembolization with a 2-F tip microcatheter for small hepatocellular carcinomas: relationship between local tumor recurrence and visualization of the portal vein with iodized oil. *J Vasc Interv Radiol* 18:365–376
9. Chung JW, Park JH, Im JG et al (1993) Pulmonary oil embolism after transcatheter oily chemoembolization of hepatocellular carcinoma. *Radiology* 187:689–693
10. Chung JW, Park JH, Han JK et al (1996) Hepatic tumors: predisposing factors for complications of transcatheter oily chemoembolization. *Radiology* 198:33–40
11. Song SY, Chung JW, Han JK et al (2001) Liver abscess after transcatheter oily chemoembolization for hepatic tumors: incidence, predisposing factors, and clinical outcome. *J Vasc Interv Radiol* 12:313–320
12. Sakamoto I, Iwanaga S, Nagaoki K et al (2003) Intrahepatic biloma formation (bile duct necrosis) after transcatheter arterial chemoembolization. *AJR Am J Roentgenol* 181:79–87
13. Yu JS, Kim KW, Park MS et al (2001) Bile duct injuries leading to portal vein obliteration after transcatheter arterial chemoembolization in the liver: CT findings and initial observations. *Radiology* 221:429–436
14. Yu JS, Kim KW, Jeong MG et al (2002) Predisposing factors of bile duct injury after transcatheter arterial chemoembolization (TACE) for hepatic malignancy. *Cardiovasc Intervent Radiol* 25:270–274
15. Sakamoto N, Monzawa S, Nagano H et al (2007) Acute tumor lysis syndrome caused by transcatheter oily chemoembolization in a patient with a large hepatocellular carcinoma. *Cardiovasc Intervent Radiol* 30:508–511
16. Makuuchi M, Sukigara M, Mori T et al (1985) Bile duct necrosis: complication of transcatheter hepatic arterial embolization. *Radiology* 156:331–334
17. Kim HK, Chung YH, Song BC et al (2001) Ischemic bile duct injury as a serious complication after transarterial chemoembolization in patients with hepatocellular carcinoma. *J Clin Gastroenterol* 32:423–427
18. Bang BW, Lee DH, Jeong S et al (2008) Ischemic biliary stricture developed after repeated transcatheter arterial chemoembolization diagnosed by percutaneous transhepatic cholangioscopy in a patient with hepatocellular carcinoma. *Gastrointest Endosc* 68:1224–1226
19. Kobayashi S, Nakanuma Y, Terada T et al (1993) Postmortem survey of bile duct necrosis and biloma in hepatocellular carcinoma after transcatheter arterial chemoembolization therapy: relevance to microvascular damages of peribiliary capillary plexus. *Am J Gastroenterol* 88:1410–1415
20. Stapleton GN, Hickman R, Terblanche J (1998) Blood supply of the right and left hepatic ducts. *Br J Surg* 85:202–207
21. Chen WJ, Ying DJ, Liu ZJ et al (1999) Analysis of the arterial supply of the extrahepatic bile ducts and its clinical significance. *Clin Anat* 12:245–249
22. Tohma T, Cho A, Okazumi S et al (2005) Communicating arcade between the right and left hepatic arteries: evaluation with CT and angiography during temporary balloon occlusion of the right or left hepatic artery. *Radiology* 237:361–365
23. Vellar ID (1999) The blood supply of the biliary ductal system and its relevance to vasculobiliary injury following cholecystectomy. *Aust N Z J Surg* 69:816–820
24. Miyayama S, Matsui O, Taki K et al (2005) Arterial blood supply to the posterior aspect of segment IV of the liver from the caudate branch: demonstration at CT after iodized oil injection. *Radiology* 237:1110–1114
25. Terayama N, Miyayama S, Tatsu H et al (1998) Subsegmental transcatheter arterial embolization for hepatocellular carcinoma in the caudate lobe. *J Vasc Interv Radiol* 9:501–508
26. Miyayama S, Mitsui T, Zen Y et al (2009) Histopathological findings after ultrasensitive transcatheter arterial chemoembolization for hepatocellular carcinoma. *Hepatol Res* 39:374–381

Inferior phrenic arteries: angiographic anatomy, variations, and catheterization techniques for transcatheter arterial chemoembolization

Shiro Miyayama · Masashi Yamashiro · Yuichi Yoshie
Miho Okuda · Yoshiko Nakashima · Hiroshi Ikeno
Nobuaki Orito · Miki Yoshida · Osamu Matsui

Received: January 17, 2010 / Accepted: April 19, 2010
© Japan Radiological Society 2010

Abstract The inferior phrenic artery (IPA) is the most common extrahepatic collateral vessel to hepatocellular carcinoma (HCC); however, there are many anatomical variations in its origin and branches. In addition, the IPA is frequently reconstructed through several pathways, mainly through the retroperitoneal network, because of the occlusion of its orifice due to atherosclerosis or previous catheter manipulation. Infrequently, selective catheterization into the IPA is impossible even using a microcatheter, particularly in the IPA that originates from the proximal or distal portion of the celiac trunk or from the aorta with an acute angle. In this article, we describe anatomical variations of the IPA and catheterization techniques, such as a catheter with a large side hole and a catheter with a cleft, to facilitate catheterization into the IPA that is difficult using a conventional coaxial technique. Radiologists should have sufficient knowledge of such variations and catheterization techniques to perform transcatheter arterial chemoembolization for HCCs through the IPA effectively and safely.

Key words Inferior phrenic artery · Anatomy · Catheterization technique · Transcatheter arterial chemoembolization

S. Miyayama (✉) · M. Yamashiro · Y. Yoshie · M. Okuda · Y. Nakashima · H. Ikeno · N. Orito · M. Yoshida
Department of Diagnostic Radiology, Fukuiken Saiseikai Hospital, 7-1 Funabashi, Wadanaka-cho, Fukui 918-8503, Japan
Tel. +81-776-23-1111; Fax +81-776-28-8519
e-mail: s-miyayama@fukui.saiseikai.or.jp

O. Matsui
Department of Radiology, Kanazawa University Graduate School of Medical Science, Kanazawa, Japan

Introduction

The inferior phrenic arteries (IPAs) are the major blood source to the diaphragm. There is close contact between the posterior portion of the liver and diaphragm at the bare area and branches of the IPA that are in direct contact with the liver.¹ In addition, the left IPA has the potential to communicate with intrahepatic arteries of the lateral segment of the liver.¹ Therefore, hepatocellular carcinoma (HCC) located near the diaphragm frequently receives its blood supply from the IPA, especially when the hepatic arterial circulation is interrupted by repeated transcatheter arterial chemoembolization (TACE) or placement of the catheter for infusion chemotherapy.^{2–4} Furthermore, IPA parasitization is also seen even at the initial TACE for tumors located bare area of the liver.^{2–5} The right IPA is the most common extrahepatic collateral supplying HCCs^{3,4}; therefore, TACE of the IPA is necessary during the subsequent course of treatment for an HCC in most cases.

The IPAs and their branches have several anatomical variations and pathological conditions,^{6,7} and several catheterization techniques are required in some cases in which the IPA has a difficult branching pattern.^{5,8–10} Therefore, radiologists should have sufficient knowledge of such variations and catheterization techniques to perform TACE through the IPA effectively and safely.

Anatomical variations of IPAs

The IPAs originate with almost equal frequency from the aorta and celiac axis, either as a common trunk or independently.⁶ These vessels may also arise from the renal (15.7%), left gastric (3.7%), hepatic (2.1%) (Fig. 1), supe-

rior mesenteric (0.3%), or spermatic arteries.⁶ In 58% of cases, the right IPA originates directly from the aorta, and the most common level of origin is the supreliac aorta, followed by the aorta between the celiac trunk and superior mesenteric artery, and the juxtaceliac aorta with the celiac trunk.¹¹ The independent right IPA USUALLY ARISES FROM THE RIGHT SIDE OF THE MAJOR ARTERY OR AORTA; however, rarely it arises from the left renal artery (Fig. 2).⁵

Variations of IPA branches

Figure 3 shows the major branches derived from the IPAs. The right and left IPAs give rise to anterior (ascending), posterior (descending), superior suprarenal, and middle suprarenal branches.

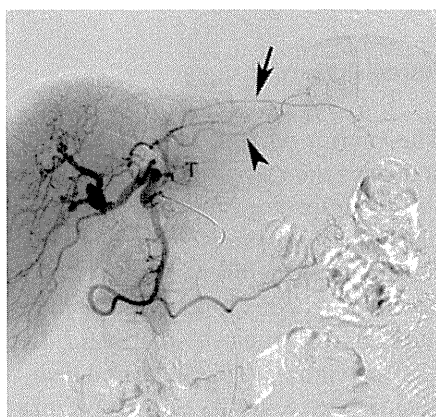


Fig. 1. Posterior branch of the left inferior phrenic artery (IPA) arises from the left hepatic artery (arrow), and the accessory left gastric artery arises from the left hepatic artery (arrowhead). Tumor stain in the caudate lobe of the liver is also seen (T)

and middle suprarenal branches. In addition, the right IPA gives rise to the inferior vena caval (Fig. 4) and diaphragmatic branches (Fig. 5); and the left IPA gives rise to gastric, esophageal (Fig. 6), and accessory splenic



Fig. 2. Right IPA arises from the left upper polar renal branch. (From Miyama et al.,⁵ with permission)

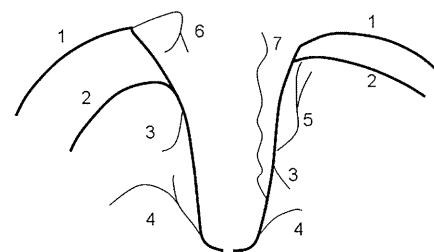


Fig. 3. Major branches derived from the IPAs. 1, anterior branch; 2, posterior branch; 3, superior suprarenal branch; 4, middle suprarenal branches; 5, gastric branch; 6, diaphragmatic branch; 7, esophageal branch

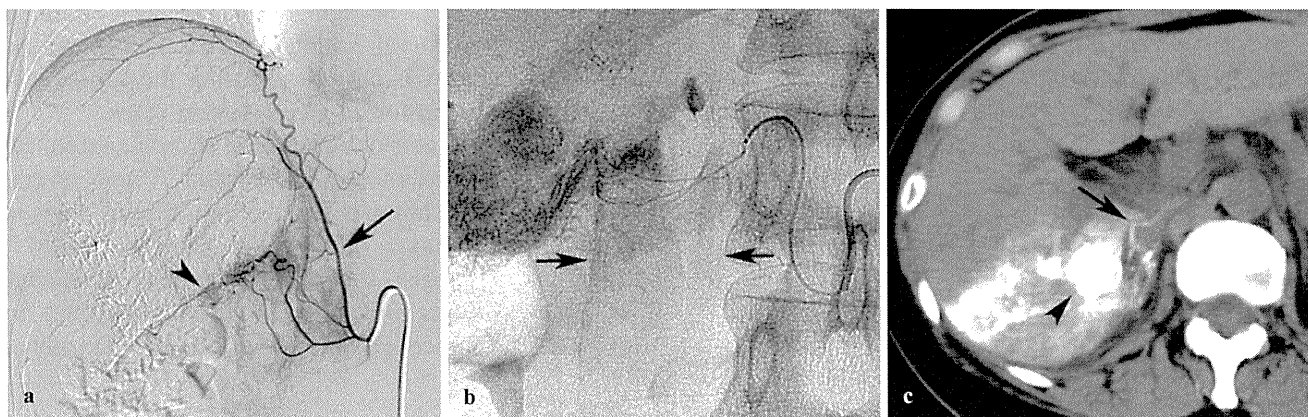


Fig. 4. a The tumor was mainly supplied by the branch of the posterior inferior subsegmental artery of the right hepatic artery, and the branch was embolized (not shown). Arteriography of the right IPA obtained after transarterial chemoembolization (TACE) of the hepatic arterial branch shows a residual tumor stain (arrowhead) supplied by a small branch (arrow). **b** The branch was selected, and TACE was performed. The branch was one of the

inferior vena caval branches, therefore, iodized oil accumulation along the inferior vena cava (IVC) was demonstrated during TACE. **c** On a computed tomography (CT) scan obtained 1 week after TACE, iodized oil accumulation is seen in the IVC wall (arrow). Iodized oil is also accumulated in the right adrenal gland because the suprarenal branch was sequentially embolized during the TACE procedure (not shown). Arrowhead indicates the tumor

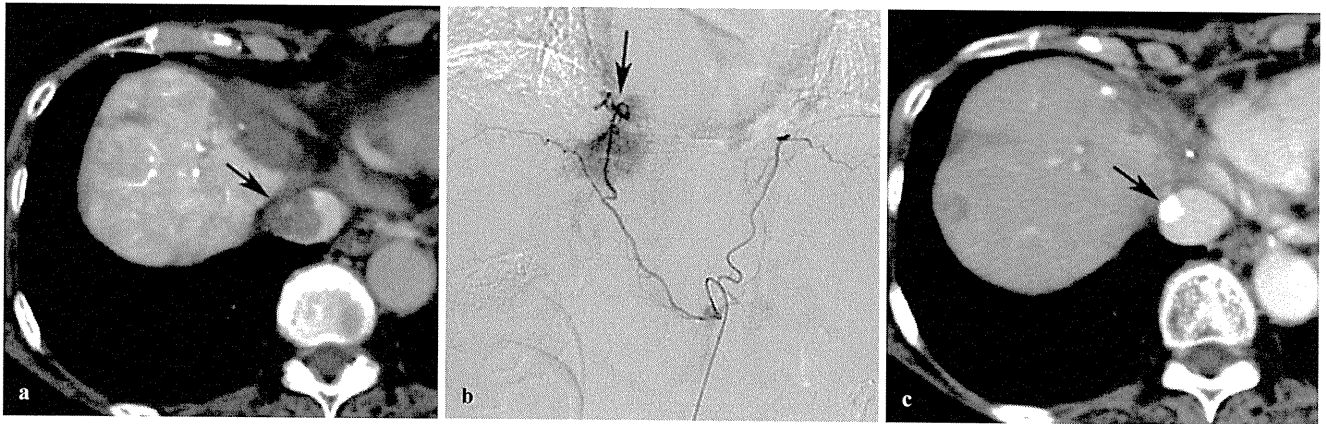


Fig. 5. **a** Computed tomography during arterial portography shows a tumor thrombus in the IVC (*arrow*). **b** Arteriography of the bilateral IPAs shows the tumor stain supplied by the diaphragmatic branch of the right IPA (*arrow*). The branch was selected,

and TACE was performed (not shown). **c** Arterial phase CT scan obtained 1 year after TACE shows that the tumor thrombus is decreased in size, with dense iodized oil accumulation

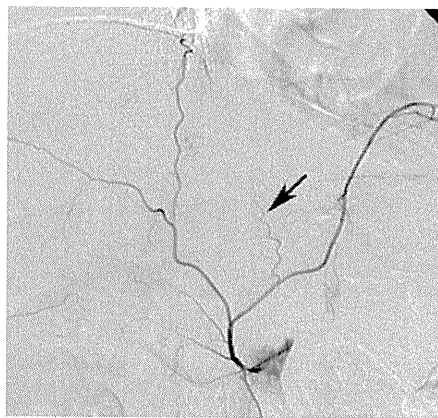


Fig. 6. Esophageal branch arises from the left IPA (*arrow*)



Fig. 7. Gastric branch (*arrow*) and left suprarenal branch (*arrow-head*) arise from the right IPA arising from the aorta

branches.^{1,6} In our experience, the gastric and esophageal branches have several anatomical variations. The gastric branch infrequently arises from the right IPA (Fig. 7) or superior mesenteric artery (Fig. 8); or it may indepen-

dently arise from the aorta (Fig. 9). In addition, anastomosis between the right IPA and the esophageal branch is also seen.

The anterior and posterior branches of the left IPA frequently arise from separate origins (Figs. 1, 10–12). The anterior branch of the left IPA frequently arises from the right IPA (Figs. 10, 11).⁷ In such a branching pattern, the posterior branch of the left IPA arises either as a common trunk (Fig. 11) or independently. In addition, the posterior branch of the left IPA infrequently arises from the left hepatic artery (Fig. 1).

Two or three inferior vena caval branches derive from the right IPA,¹² and these branches supply HCCs adjacent to the inferior vena cava (IVC) (Fig. 4). The inferior vena caval and diaphragmatic branches are also the major blood source to the tumor thrombus of an HCC in the IVC (Fig. 5).¹³

The right IPA communicates with the pericardiaco-phrenic artery arising from the right internal mammary artery. A vascular blush caused by transpleural systemic–pulmonary arterial anastomosis from the IPA is frequently seen in patients with chronic pleural and/or pulmonary inflammation (Fig. 13).⁶

Variations of reconstructed pathways of occluded IPAs

Stenosis or occlusion of the orifice of the IPA may occur owing to atherosclerotic change or previous catheter manipulation.¹⁴ Arcuate ligament compression may also cause stenosis or occlusion of the IPA orifice. The IPA has many anastomoses between the contralateral IPA, internal mammary, posterior intercostal and lumbar, left gastric, dorsal pancreatic, and adrenal arteries; therefore, it is reconstructed from various vessels when the

Fig. 8. **a** Bilateral IPAs arise from the celiac trunk. The gastric branch is not derived from the left IPA. **b** Gastric branch arises from the superior mesenteric artery

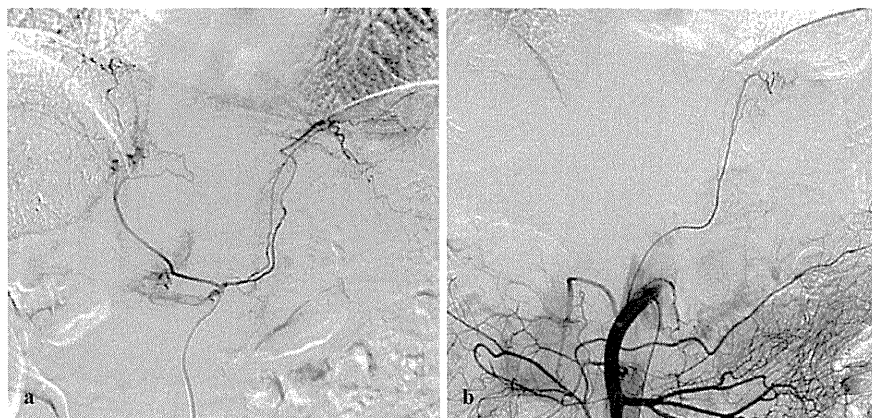


Fig. 9. **a** Bilateral IPAs directly arise from the aorta. The gastric branch is not derived from the left IPA. **b** Gastric branch independently arises from the aorta

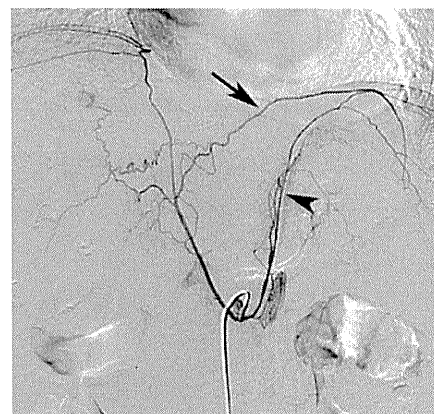
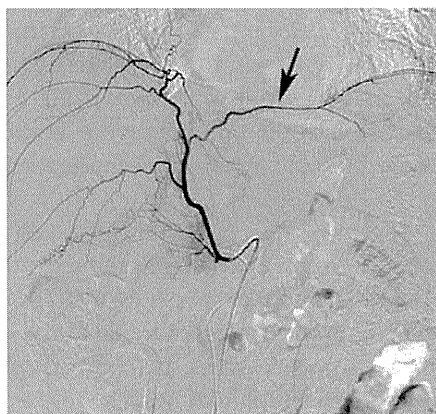
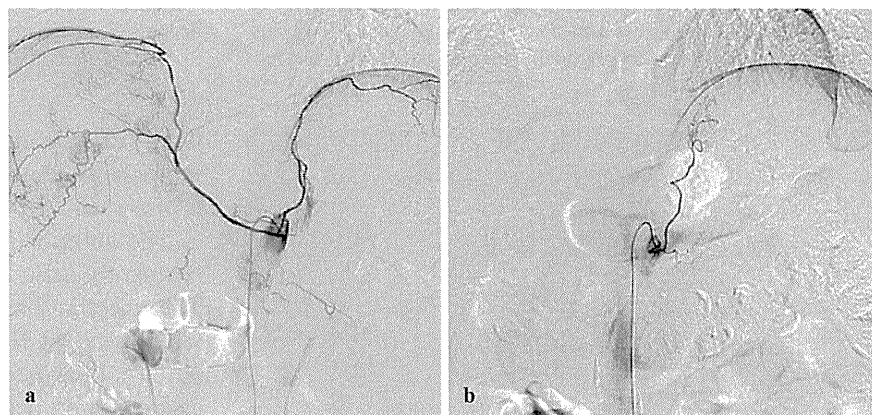


Fig. 10. Anterior branch of the left IPA arises from the right IPA (arrow)

Fig. 11. Anterior branch of the left IPA arises from the right IPA (arrow). Posterior branch of the left IPA arises with a common trunk (arrowhead)

orifice is occluded (Figs. 14–18).^{5,6,14,15} The occluded IPA is mainly opacified through the retroperitoneal network; the dorsal pancreatic artery is the most common collateral to the IPAs (Figs. 14, 15), followed by the right adrenal arteries (Fig. 16), left gastric artery (Figs. 14, 15), and contralateral IPA.¹⁴ The IPAs are also reconstructed through an unnamed small branch arising from the celiac trunk (Fig. 17) or renal artery (Fig. 18). In addition,

the IPAs are frequently opacified through more than two individual arteries (Fig. 14, 15).¹⁴

Catheterization technique into IPAs

With advances in the technology of catheters and guidewires, almost all IPAs can be selected.⁴ However, cath-